Modern Physics Letters B
Vol. 31, No. 16 (2017) 1750167 (11 pages)

DOI: 10.1142/S0217984917501676

World Scientific
www.worldscientific.com

Numerical experiments on the PF1000 plasma focus device operated with nitrogen and oxygen gases

M. Akel*,**, Sh. Ismael*, S. Lee†,‡,§, S. H. Saw†,¶ and H. J. Kunze‖

*Department of Physics, Atomic Energy Commission, Damascus, P. O. Box 6091, Syria
†Institute for Plasma Focus Studies, 32 Oakpark Drive, Chadstone, VIC 3148, Australia
‡University of Malaya, Kuala Lumpur, Malaysia
§INTI International University, 71800 Nilai, Malaysia
¶Nilai University, 1, Persiaran University, Putra Nilai, 71800 Nilai, Malaysia
‖Institute for Experimental Physics V, Ruhr-University Bochum, Germany
**pscientific@aec.org.sy

Received 15 January 2017
Revised 23 March 2017
Accepted 31 March 2017
Published 30 May 2017

The indicative values of reduced Pease–Braginskii (P–B) currents are estimated for a nitrogen and oxygen plasma focus. The values of depletion times indicate that in N_2 and O_2 with estimated 3–4% of pinch energy radiating away over the duration of the pinch, we may expect some cooling effects leading to small reductions in radius ratio. In other gases with higher atomic number, the pinch duration is much more than the depletion time, so radiative contraction may be anticipated. The Lee model was employed to study the soft X-ray from PF1000 operated with nitrogen and oxygen. We found nitrogen soft X-ray yield in the water window region of 3.13 kJ, with the corresponding efficiency of 0.9% of the stored energy (E_0), while for the oxygen it was found to be $Y_{\mathrm{sxr}} = 4.9$ kJ, with the efficiency of 1.4% E_0. The very modest enhancement of compression (radius ratios around 0.1) in the pinches of these two gases gives rise to rather modest pinch energy densities (PEDs) under 10^9 Jm^{-3}. This is in contrast to Kr or Xe where it had been shown that the radiative collapse leads to radius ratios of 0.007 and 0.003, respectively, with PEDs going to large values considerably exceeding 10^{12} Jm^{-3}.

Keywords: Lee model; soft X-ray; pinch radius; radiative contraction; N_2 and O_2 gases.

1. Introduction

Pinch plasmas are highly brilliant sources of thermal radiation in the soft X-ray range. The plasma energy is increased by the pinch effect, attaining higher ionization states. A large amount of its energy is converted into soft X-radiation mainly

**Corresponding author.

by radiative recombination and line emission.[1] The plasma focus (PF)[2,3] is arguably the simplest yet provides the highest X-ray emission[4,5] among the other various types of pinches such as Z-pinch,[6] X-pinch,[7] and vacuum spark.[8,9] Nitrogen is used for soft X-rays,[10–12] and PF devices operated with nitrogen are sources for X-ray microscopy.[13,14] Similarly, PF machines operated in oxygen are used to emit soft rays suitable for water-window microscopy,[15] and as an ion source for material science applications.[16] The Lee model code was modified to include nitrogen and oxygen gases. The suitable temperature range for generating H-like (Ly_α (1s–2p, N_2: 2.478 nm)) and He-like (He_β($1s^2$–1s3p, N_2: 2.496 nm)) ions in nitrogen plasma was found to be 74–173 eV (0.86×10^6–2×10^6 K). For oxygen the temperature (Te) range for H-like (1s–2p, O2: 1.897 nm) and He-like ($1s^2$–1s2p, O2: 2.16 nm) ions was 119–260 eV (1.38×10^6–3×10^6 K). So we take the soft X-ray yield to be equivalent to line radiation yield at the suitable temperature range[17] for each of these two gases. The Pease–Braginskii (P–B) current $I_{\text{P–B}}$[18–21] is the electric current which is just large enough for the bremsstrahlung in a pinch to balance Joule heating. For a strongly radiating gas, the radiation-cooled threshold current is lowered. The equations of the Lee model code compute this lowering.[18] The neutron enhancement effect of krypton seeding had also been ascribed to enhanced compression caused by radiation.[22] Ali *et al.*[23] reported that self-absorption becomes significant when the plasma is optically thick due to increased density. Recently, reduced Pease–Braginskii currents ($I_{\text{P–B reduced}}$) are estimated for D_2, He, Ne, Ar, Kr and Xe. A characteristic depletion time for PF pinch energy was defined as an indicator for probability of radiative collapse. These indicate that in D_2 and He, no radiative collapse may be expected. In Ne, low tens of percent are radiated, hence cooling and reduction in the radius may be expected. In Ar, Kr and Xe, the strong radiative collapse is expected.[21] Measured results of the PF1000 operated in neon were also reported and compared with the results of the Lee code.[24] In this work, the Lee code is utilized on PF1000 operated with nitrogen and oxygen filling gases to study the pinch dynamics and radiative collapse and to characterize the nitrogen and oxygen soft X-ray yields from PF1000.

2. Numerical Experiments on PF1000: Results and discussion

Following Ref. 21, we estimate typical values of $I_{\text{P–B reduced}}$ for nitrogen and oxygen gases as follows:

$$I^2_{\text{P–B reduced}} = I_{\text{P–B}^2} \times \frac{1}{K} \times Z', \quad \text{where} \quad Z' = (1/4)\frac{(1+Z_{\text{eff}})^2}{Z^2_{\text{eff}}},$$

$$K = \left[\frac{(dQ_{\text{line}}/dt) + (dQ_{\text{Brem}}/dt)}{(dQ_{\text{Brem}}/dt)}\right],$$

Z_{eff} — effective charge number, dQ_{line}/dt and dQ_{Brem}/dt are the line radiation and bremsstrahlung powers, respectively.

Table 1. Reduced Pease–Braginskii current for various gases; typical PF operating conditions. Where b = cathode radius, a = anode radius, z_0 = anode length, V_0 = operating voltage, p_0 = gas pressure, $I_{\text{P–B reduced}}$ = reduced Pease–Braginskii currents, T = pinch temperature.

Gases	b (cm)	a (cm)	z_0 (cm)	V_0 (kV)	p_0 (mbar)	$I_{\text{P–B reduced}}$ (kA)	T ($\times 10^6$ K)
D_2	16	11.55	150	56.3	4	1562	4.3
He	16	11.55	100	42	2.7	1175	4.8
N_2	2.1	1.5	100	6	1.6	239	3.6
O_2	2.1	1.5	100	5.4	1.13	214	4
Ne	2.1	1.5	100	5	0.54	187	9.0

As an example for N_2, we take a typical point of operation for intense line radiation at $Z_{\text{eff}} \sim 6$. At this point of operation dQ_{line}/dt is found to be 15.52 dQ_{Brem}/dt; so we have $I_{P-B\text{reduced}} \sim 239$ kA. Unlike for H_2 or D_2, when higher atomic number gases are considered with line radiation, there is no unique value for the $I_{\text{P–B reduced}}$. Thus Table 1 gives only indicative values of $I_{\text{P–B reduced}}$ with the trend that as the atomic number increases, a lower value of $I_{P-B\,\text{reduced}}$ may be expected.

The net depletion time (t_Q) is defined as the time it takes for the PF pinch energy to be radiated away ($t_Q = E_{\text{pinch}}/(dQ/dt)$, where E_{pinch} is the thermal energy in the pinch and $dQ/dt = (dQ_{\text{line}}/dt) + (dQ_{\text{Brem}}/dt) - P_J$ (P_J is the Joule heating)[21] is calculated and also t_Q^* (which is t_Q expressed in units of a characteristic pinch time τ_{pinch}). Table 2 shows sample computations of effective charge number (Z_{eff}), specific heat ratio (SHR), pinch current I_{pinch} and depletion times in D_2, He, N_2, O_2 and Ne for some conditions shown to be practicable PF operation in the numerical experiments.

The pinch time is proportional to anode radius with a value of 10 ns per cm.[25] From Table 2 it is noted that even though the PF operates above the reduced P–B, there would be no radiative collapse to be expected from operation in H_2 and He; nor perhaps in N_2 (with estimated 3% of pinch energy radiated away over the duration of the pinch we may expect some cooling effects leading to small reduction in radius ratio). As already discussed in Ref. 21 in Ne with significant proportion of pinch energy radiated away within one τ_{pinch}, radiative cooling should be expected, leading to considerable reduction in minimum radius ratio. In Ar, Kr and Xe strong radiative collapse is expected.

Table 2. Computed net depletion times for various conditions.

Gas	b (cm)	a (cm)	z_0 (cm)	V_0 (kV)	p_0 (mbar)	I_{pinch} (kA)	Z_{eff}	SHR	t_Q (s)	t_Q^* (τ_{pinch})
D_2	28	20	60	90	4.7	2125	1.0	1.67	3.2E-03	32000
He	27.8	20	60	90	4.7	2094	2.0	1.64	8.8E-05	880
N_2	7	5	60	14	1.33	529	6.2	1.47	1.5E-06	15
O_2	7	5	60	14	1.33	527	7.22	1.45	6E-07	6
Ne	7	5	60	14	1.33	514	8.3	1.49	2.6E-07	2.6

We next carry out numerical experiments on PF1000 operated with nitrogen and oxygen filling gases using the code in which $Q, dQ/dt$ (or Qdot) and plasma self-absorption effect are all included.[26–28] We used the following configuration for the PF1000:

Bank parameters: $L_0 = 33$ nH (fitted), $C_0 = 1332$ μF, $r_0 = 3$ mΩ (fitted), (where L_0 = static inductance (nominal), C_0 = storage capacitance (nominal) and r_0 = stray circuit resistance).

Tube parameters: $b = 16$ cm, $a = 11.55$ cm, $z_0 = 60$ cm, (b = cathode radius, a = anode radius, z_0 = anode length). Operating parameters: $V_0 = 23$ kV, $p_0 = 2$ mbar and gas parameters (for deuterium) are 4 (molecular weight), 1 (atomic number) and 2 (molecular gas).

Together the following model parameters[29,30]: $f_{\mathrm{m}} = 0.11$, $f_{\mathrm{c}} = 0.7$, $f_{\mathrm{mr}} = 0.26$, $f_{\mathrm{cr}} = 0.68$, (where the mass swept-up factor f_{m}, the plasma current factor f_{c} for the axial phase and the mass swept-up factor f_{mr} and the plasma current factor f_{cr} for the radial phases).

We use these model parameters and the above mentioned configuration for a new series of numerical experiments on nitrogen and oxygen.

2.1. *PF1000 operated with nitrogen*

Figure 1 shows the total discharge current rising to a peak value of 2064 kA. The pinch current I_{pinch} at start of pinch (time of start of pinch is shown in the Fig. 1 with the right-pointing arrow). Figure 2 shows the trajectories in the radial phase and the net radiation power in PF1000 PF at 23 kV, 1.33 mbar at nitrogen filling gas. The piston trajectory delineates the pinch radius after the piston meets the reflected shock (RS). For this shot, the pinch lasts for 232 ns. The code computes the radial trajectory up to this point. Figure 2 shows a very slow compression (i.e. radius decreases barely perceptibly), typical of an efficiently-operated pinch with no radiation compression or significant cooling. The increasing effect of the radiation terms as Z increases is shown in the case of N_2 in which the minimum radius of the

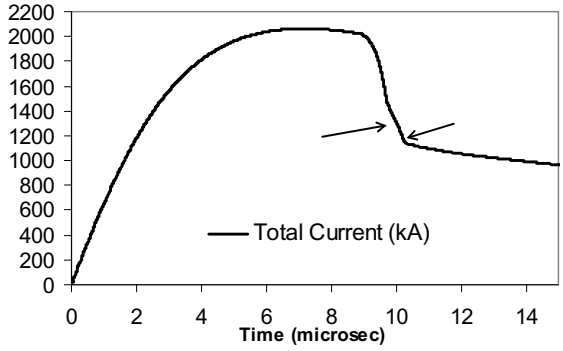

Fig. 1. Computed total current of the PF1000 at 23 kV, 1.33 mbar at nitrogen filling gas.

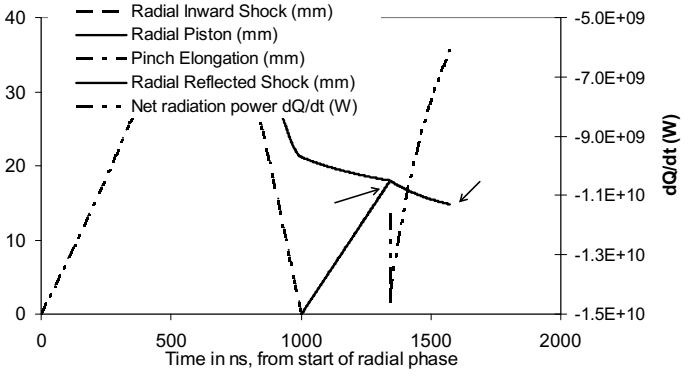

Fig. 2. Radial inward shock, radial piston, radial reflected shock, pinch elongation and net radiation power in PF1000 PF.

pinch is now computed as 1.48 cm as seen in the increased compression in Fig. 2 for the radial trajectory of N_2. A study of the various output terms from the code again supports the trend as shown in Table 2. Figure 2 also shows the period of time (1000–1800 ns) covering the radial phase together with dQ/dt which is the radiation power emitted from the pinch minus the Joule heating power. This is the term responsible for radiative collapse if negative and sufficiently large in value.

At this start of the radial phase, the total circuit current is 2030 kA whilst the pinch current is 1378 kA. In the first hundreds of nanoseconds of the radial phase, the radial shock front SF moves towards the axis driven by the piston with an annular slug of plasma between the SF and the piston. The shock front hits the axis at 1000 ns and because the conditions are collisional, a reflected shock RS forms and moves radially outwards whilst the piston continues to move radially towards the axis. The RS hits the piston (at 1343 ns) at radial position of 1.8 cm (see Fig. 2). This is the start of the ("normally" slow-compression phase when radiative collapse is excluded) pinch phase (indicated in Fig. 2 by the first arrow which is right-pointing). In this case of N_2 the pinch current is 866 kA and the conditions are such that the value of the net radiative power $dQ/dt = 11.6 \times 10^9$ W, which is enough to start a rapid compression of the pinch. The power dQ/dt then increases as the compression proceeds rising to a peak value of 14×10^9 W at 1344 ns. The code shows an absorption coefficient of 0.3 at this time of peak Qdot and with absorption continuing to increase rapidly. The pinch has a radius of 1.78 cm. Even as the power Qdot decreases, the compressions continues until minimum radius of 1.48 cm is reached at a time of 1580 ns when Qdot has dropped to 6.1×10^9 W. At this time, the pinch current is 782 kA. The value of Q is 2.2 kJ which is about 2.8% of the pinch energy (EINP) of 79 kJ. Dividing the pinch energy by the pinch volume, the pinch energy density (PED) is computed as 6.3×10^8 Jm^{-3}. These fitted model parameters are then used for the computation of the discharges at various pressures from 0.3 mbar to 4 mbar in N_2. From the obtained results (Table 3), it is seen that

Table 3. Variation of nitrogen pinch parameters with pressure in PF1000.

p_0 (mbar)	I_{peak} (kA)	I_{pinch} (kA)	T_{max} ($\times 10^6$ K)	r_p (cm)	Z_{max} (cm)	Pinch dur. (ns)	Y_{sxr} (J)	EINP (J)	PED ($\times 10^8$ Jm^{-3})
0.27	1620	727	4.66	1.80	18.1	139.0	98.80	47436.16	2.58
0.53	1817	803	2.84	1.65	18.2	167.8	870.17	61064.74	3.92
0.80	1926	839	2.29	1.46	18.3	190.8	2462.87	70236.24	5.75
0.93	1968	850	2.05	1.39	18.4	201.3	3130.82	73718.31	6.63
1.07	2004	857	1.86	1.40	18.4	212.4	3012.76	76049.69	6.70
1.20	2036	863	1.70	1.45	18.3	221.8	2495.63	77580.73	6.40
1.33	2064	866	1.55	1.48	18.3	231.9	2186.52	79063.07	6.30
1.47	2089	867	1.43	1.52	18.2	241.9	1712.34	80107.37	6.06
1.60	2112	868	1.33	1.55	18.2	251.0	1345.13	81013.79	5.92
1.87	2152	866	1.15	1.58	18.2	270.5	857.95	82558.29	5.79
2.13	2186	861	1.00	1.59	18.1	290.8	525.34	83721.91	5.78
2.40	2216	853	0.89	1.60	18.1	307.4	121.68	84423.84	5.80
2.67	2242	843	0.79	1.60	18.1	325.3	0.00	84817.13	5.83
2.93	2266	832	0.70	1.60	18.1	343.7	0.00	84929.67	5.85
3.20	2287	819	0.63	1.59	18.1	361.3	0.00	84775.78	5.92
3.73	2324	791	0.51	1.55	18.0	395.8	0.00	83760.79	6.16
4.00	2341	775	0.46	1.53	18.0	415.1	0.00	82994.13	6.26

the Y_{sxr} increases with increasing pressure until it reaches the maximum value about 3.13 kJ at $p_0 = 0.9$ mbar (with the corresponding efficiency being about 0.9% E_0), after which it decreases with higher pressures.

As expected as p_0 is increased, the end axial speed, the inward shock speed and the radial piston speed are reduced. The decrease in speeds leads to a lowering of the plasma temperatures below that needed for soft X-ray production (see Fig. 3). From Table 3, it can be seen that, for the nitrogen PF the radius drops with increasing operating pressure, until it reaches a minimum value of 1.39 cm at 0.9 mbar, while at this point the pinch length has a maximum value of 18.4 cm. The maximum value of EINP is 85 kJ (24% E_0) at 3 mbar, while the PED reaches a maximum value of 6.7×10^8 Jm^{-3} at lower pressure of 1.1 mbar (see Fig. 4).

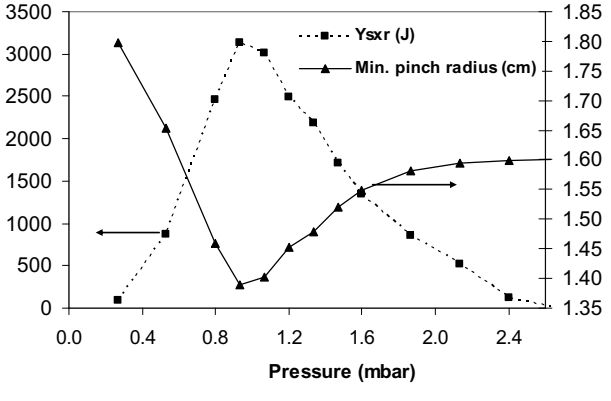

Fig. 3. Soft X-ray yield and minimum pinch radius versus nitrogen pressure in PF1000 PF.

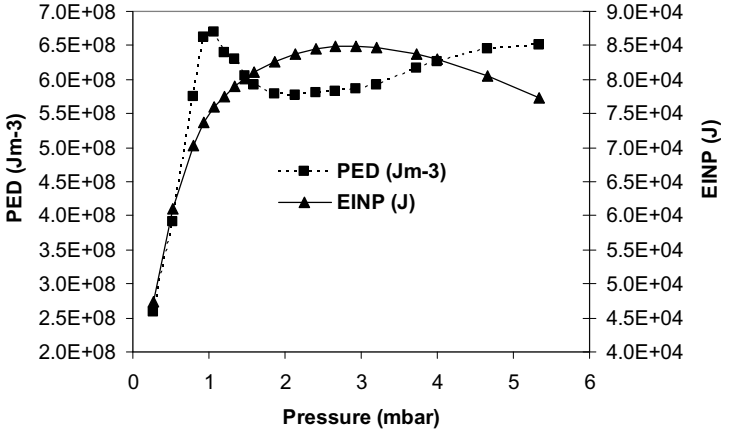

Fig. 4. Pinch energy EINP and the pinch energy density (PED) versus nitrogen pressure in PF1000 PF.

2.2. *PF1000 operated with oxygen*

The increasing effect of the radiation terms as Z increases is shown in the case of O_2 in which the minimum radius of the pinch is now computed as 1.39 cm. Figure 5 shows the total discharge current rising to a peak value of 2100 kA. Figure 6 shows the trajectories in the radial phase and the net radiation power in PF1000 PF at 23 kV, 1.33 mbar at oxygen filling gas. The piston trajectory delineates the pinch radius after the piston meets the RS. For this shot, the pinch lasts for 242 ns. Figure 6 shows a very slow compression typical of an efficiently-operated pinch with no radiation compression or significant cooling. At this start of the radial phase, the total circuit current is 2050 kA whilst the pinch current is 1400 kA. The shock front hits the axis at 1080 ns and the RS hits the piston at 1390 ns at radial position 1.65 cm. This is the start of the pinch phase (see Fig. 6). In this case of O_2 the pinch current is 848 kA and the conditions are such that the

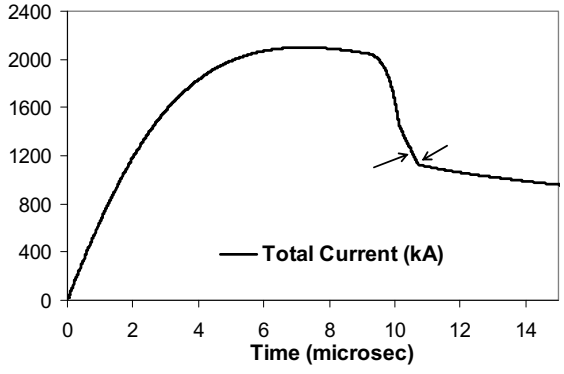

Fig. 5. Computed total current of the PF1000 at 23 kV, 1.33 mbar at oxygen filling gas.

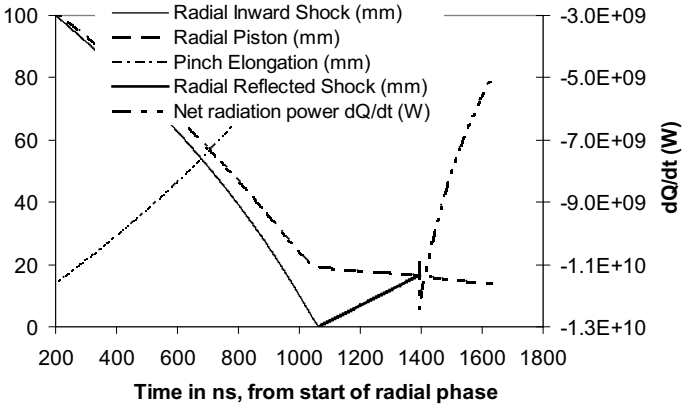

Fig. 6. Radial dynamics and net radiation power in PF1000 PF at 23 kV, 1.33 mbar at oxygen filling gas.

value of the net radiative power $dQ/dt = 10.9 \times 10^9$ W, which is enough to start a rapid compression of the pinch. The power dQ/dt then increases as the compression proceeds rising to a peak value of 12.4×10^9 W at 1400 ns.

The code shows an absorption coefficient of 0.035 at this time of peak Qdot with absorption continuing to increase rapidly. The pinch has a radius of 1.65 cm. Even as the power Qdot decreases, the compression continues until minimum radius of 1.39 cm is reached at a time of 1640 ns when Qdot has dropped to 4.93×10^9 W. At this time, the pinch current is 767 kA. The operating pressure was varied from 0.27 mbar to 6.7 mbar. The Y_{sxr} increases with increasing pressure until a maximum of 4.9 kJ at 0.8 mbar (efficiency of 1.4% E_0), after which it decreases with higher pressures (see Fig. 7). At this pressure, the O_2 pinch is near optimum compression

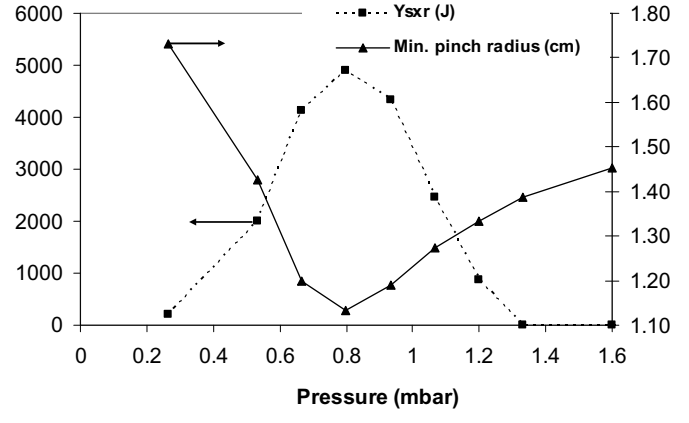

Fig. 7. Soft X-ray yield and minimum pinch radius versus oxygen pressure in PF1000 PF.

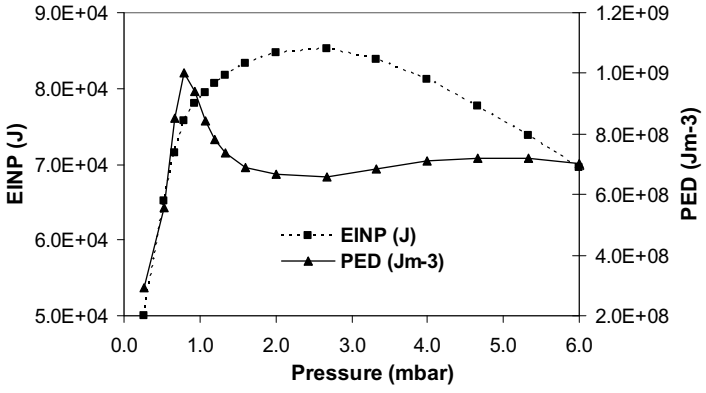

Fig. 8. Pinch energy EINP and the PED versus oxygen pressure in PF1000 PF.

Table 4. Summary of numerical experiments of PF1000 (with $E_0 \sim 352.3$ kJ) radiative collapse in various gases.

Gas	p_0 (mbar)	I_{ps} (kA)	I_{pe} (kA)	t_{min} (ns)	t_p (ns)	r_{ps} (mm)	k_{min} (r_p/a)	$-Q\text{dot}_{peak}$ (10^{11} W)	$-Q$ (% E_0)	$-E_{rad}$ (% E_0)	EINP (% E_0)	PED (Jm^{-3})
D_2	4	853	789	206	206	23.8	0.192	−0.0005	−0.00002	0.000003	17.0	2.14×10^8
He	4	833	768	190	190	21.9	0.178	0.0008	0.00004	0.00008	17.2	2.51×10^8
N_2	0.9	866	782	201	201	18.5	0.12	0.15	0.9	0.98	21	6.6×10^8
O_2	0.8	850	770	200	200	17.4	0.1	0.18	1.4	1.53	22	1×10^9
Ne	1.13	810	626	222	222	16.2	0.058	0.23	2.93	3.15	23	2.73×10^9

I_{ps} = plasma current at start of pinch, I_{pe} = plasma current at end of pinch, t_{min} = time to min radius, t_p = time to end of pinch, r_{ps} = pinch radius at start of pinch, k_{min} = min radius ratio r_{min}/a, $-Q\text{dot}_{peak}$ = peak value of $-dQ/dt$, Q = energy radiated from pinch less Joule heat energy deposited in pinch; E_{rad} = energy radiated for whole pinch duration in terms of storage energy E_0, EINP = pinch energy, PED = pinch energy density.

with a pinch energy of 76 kJ and an energy density of 10×10^8 Jm^{-3}. The obtained results also show that the radius drops with increasing operating oxygen pressure, until it reaches a minimum value of 1.13 cm at 0.8 mbar, while at this point the pinch length has the maximum value of 18.8 cm. The maximum value of EINP is 85.2 kJ (24.2% E_0) at 2.7 mbar, while the PED reaches a maximum value of 10×10^8 Jm^{-3} at pressure of 0.8 mbar near optimum compression (see Fig. 8).

The data are summarized in Table 4. In this table, the values of peak $-Q\text{dot}$, $-Q$ and $-E_{rad}$ are shown. Positive values in the $-Q\text{dot}$ and $-Q$ columns indicate that the radiation exceeds the Joule heating in the pinch so that the net power works in the direction of radiation cooling and collapse. The values of these two quantities for D_2 are negative indicating that Joule heating exceeds radiation. The He pinch does show a perceptible increased compression of the pinch with pinch radius ratio k_{min} of 0.178 compared to that of D_2 of 0.192, although the power is small and the heat loss is such a small percentage of the pinch energy. The obtained results show that the radiative cooling could start in the pinch N_2 plasma with k_{min}

of 0.12 and in O_2 with $k_{\min}$ of 0.1, and is expected to be stronger with the higher Z gases. Finally, we would like to emphasize that the code assumes the pinch is compressed as a column. In actual operation, break-up of the column into a line of spots has been observed particularly, but not exclusively in the heavier gases.[31] Such break-ups may lead to localized enhanced compression and may tend to make it easier for radiative collapse to occur. Moreover, the action of beams will also remove energy from the pinch.[32,33] If beams are emitted even partially within the pinch time, this could also lead to beam-enhanced radiative collapse.

3. Conclusion

In this paper, we derive indicative values of $I_{P-B\,\text{reduced}}$ for nitrogen and oxygen as well as for various gases. We derive radiation levels and estimate characteristic depletion times of pinch energy due to radiation minus Joule heating. The results give that the PF1000 operated in D_2 and He will have little or no radiation cooling; whilst operated in N_2 and O_2 will show small radiation cooling leading to appreciable radiative compression. Operation in Ne will show significant radiation cooling leading to substantial radiative compression. These results (Tables 1 and 2) are estimated without considering plasma opacity (plasma self-absorption). The numerical experiments, which include self-absorption demonstrate substantial moderating effects of self-absorption, nevertheless confirm the indications of these two tables. The Lee model is used to calculate the X-ray yield from PF1000 operated with nitrogen and oxygen, finding a maximum nitrogen soft X-ray yield in the water-window region of 3.13 kJ (0.9% E_0). For oxygen, the maximum yield is 4.9 kJ (1.4% E_0). The very modest enhancement of compression (radius ratios around 0.1) in the pinches of these two gases gives rise to rather modest PEDs under 10^9 Jm^{-3}. This is in contrast to Kr or Xe where the radiative collapse leads to radius ratios of 0.007 and 0.003, respectively, with PEDs going to large values considerably exceeding 10^{12} Jm^{-3}.[21] Recent measurements[34] in a small PF operated at 2 kJ confirm that even in a small PF, energy densities considerably exceeding 10^{12} Jm^{-3} are achieved in Kr. This study complements the earlier paper[21] and further underlines the differences to be expected in studying the range of gases from the viewpoint of radiative cooling and collapse.

Acknowledgment

M. Akel and Sh. Ismael would like to thank Director General of AECS, for encouragement and permanent support.

References

1. R. Lebert, D. Rothweiler, A. Engel, K. Bergmann and W. Neff, *Opt. Quantum Electron.* **28** (1996) 241.
2. J. W. Mather, *Phys. Fluids* **8** (1965) 366.
3. M. Zakaullah *et al.*, *Phys. Plasmas* **6** (1999) 3188.

4. M. Zakaullah *et al.*, *Appl. Phys. Lett.* **78** (2001) 877.
5. S. Lee *et al.*, *IEEE Trans. Plasma Sci.* **26** (1998) 1119.
6. V. L. Kantsyrev *et al.*, *Proc. 3rd Int. Conf. on Dense Z-pinches* (London, UK), Vol. 299, eds. M. Haines and A. Knight (AIP, New York, 1993), 226pp.
7. D. A. Hammer *et al.*, *Appl. Phys. Lett.* **57** (1990) 2083.
8. A. Ikhlef *et al.*, *Proc. 3rd Int. Conf. on Dense Z-pinches* (London, UK), Vol. 299, eds. M. Haines and A. Knight (AIP, New York, 1993), 218pp.
9. C. S. Wong and S. Lee, *Rev. Sci. Instrum.* **55** (1984) 1125.
10. M. Shafiq *et al.*, *Mod. Phys. Lett. B* **16** (2002) 309.
11. N. K. Neog *et al.*, *J. Appl. Phys.* **99** (2006) 013302.
12. A. Roomi *et al.*, *J. Fusion Energy* **30** (2011) 413.
13. F. Richer *et al.*, *Proc. 2nd Int. Conf. Dense Z-pinches*, Vol. 195 (AIP, New York, 1989), 515pp.
14. R. Lebert, A. Engel and W. Neff, *J. Appl. Phys.* **78** (1995) 6414.
15. R. Lebert, W. Neff and D. Rothweiler, *J. X-Ray Sci. Technol.* **6** (1996) 107.
16. L. Rico, B. J. Gomez, J. N. Feugeas and O. de Sanctis, *Appl. Surf. Sci.* **254** (2007) 193.
17. M. Akel, S. Lee and S. H. Saw, *IEEE Trans. Plasma Sci.* **40** (2012) 3290.
18. S. Lee, S. H. Saw and J. Ali, *J. Fusion Energy* **32** (2013) 42.
19. M. Akel and S. Lee, *J. Fusion Energy* **32** (2013) 111.
20. M. Akel, S. Lee and S. H. Saw, *IEEE Trans. Plasma Sci.* **40** (2012) 3290.
21. S. Lee, S. H. Saw, M. Akel, J. Ali, H.-J. Kunze, P. Kubes and M. Paduch, *IEEE Trans. Plasma Sci.* **44** (2016) 165.
22. S. Lee and S. H. Saw, Multi-radiation modelling of the plasma focus, in *5th Int. Conf. Frontiers of Plasma Physics and Technology*, 18–22 April 2011, Singapore.
23. Z. Ali, S. Lee, F. D. Ismail, I. Saktioto, J. Ali and P. P. Yupapin, *Phys. Procedia* **8** (2011) 393.
24. M. Akel, J. Cikhardt, P. Kubes, H.-J. Kunze, S. Lee, M. Paduch and S. H. Saw, *Nukleonika* **61** (2016) 145.
25. S. Lee, *Aust. J. Phys.* **36** (1983) 891.
26. S. Lee, http://www.plasmafocus.net.
27. S. Lee, *J. Fusion Energy* **33** (2014) 319.
28. N. A. D. Khattak, Anomalous heating (LHDI) (2011), http://www.plasmafocus.net/IPFS/modelpackage/File3Appendix.pdf.
29. Sh. Al-Hawat, M. Akel, S. Lee and S. H. Saw, *J. Fusion Energy* **31** (2012) 13.
30. S. Lee *et al.*, *J. Fusion Energy* **33** (2014) 235.
31. F. N. Beg, I. Ross, A. Lorenz, J. F. Worley, A. E. Dangor and M. G. Haines, *J. Appl. Phys.* **88** (2000) 3225.
32. S. Lee and S. H. Saw, *Phys. Plasmas* **19** (2012) 112703.
33. S. Lee and S. H. Saw, *Phys. Plasmas* **20** (2013) 062702.
34. S. H. Saw and S. Lee, *J. Fusion Energy* **35** (2016) 702.